

CCD photometry of galactic open star clusters—III. NGC 1931

B. C. Bhatt, A. K. Pandey, H. S. Mahra and D. C. Paliwal

Uttar Pradesh State Observatory, Manora Peak, Naini Tal 263 129

Received 1993 August 27, accepted 1993 November 12

Abstract. CCD photometric observations of young open cluster NGC 1931 in *UBVRI* passbands have been made down to 20.5 mag. The reddening across the cluster is found to be variable. The reddening varies from $E(B - V)_{\min} = 0.55$ mag to $E(B - V)_{\max} = 1.00$ mag. A distance of 2.17 kpc, an age of $\sim 10^7$ yr and luminosity function for the cluster have also been derived. The luminosity function has been compared with the luminosity function of other young clusters.

Key words : open cluster—photometry

1. Introduction

The young open cluster NGC 1931 (C0528 + 342) ($l = 173^\circ.9$, $b = +0^\circ.28$) is situated in the spiral arm which is an extension of the Perseus arm (Moffat *et al.* 1979; Pandey & Mahra 1986). Moffat *et al.* (1979) have obtained photometric magnitudes of four stars in the cluster field. Pandey & Mahra (1986) have obtained the photoelectric magnitudes for 27 stars in the cluster region and discussed reddening across the cluster, its distance and age. Trumpler class I 3 p has been assigned to the cluster in the catalogue of Lynga (1987). The faint members of this poor cluster have not been studied before, but with the advent of charge couple devices (CCD) it is now possible to study such faint cluster members even with a moderate sized (~ 1 -metre class) telescope.

The aim of the present study is to describe the *UBVRI* CCD photometric observations of the stars in the field of NGC 1931 and to compare the results with those obtained by Pandey & Mahra (1986). Since the cluster is a young one, present observations give us an opportunity to study the luminosity function (LF) and subsequently we expect to gain insight into the star formation process itself by comparing the luminosity function of NGC 1931 with similar young clusters.

2. Observations

The observations of NGC 1931 were carried out in the *U*, *B*, *V*, *R* and *I* passbands using the Photometrics CCD system having a 384×576 pixels Thomson chip, at $f/13$ Cassegrain

focus of the 104-cm reflector of the Uttar Pradesh State Observatory (UPSO) during December 1991, November 1992 and January 1993. In this set up the entire CCD chip covers a field of 2.0×3.0 sq arc-min of the sky. In order to improve the S/N ratio the observations were taken at 2×2 binning mode. The details of the present CCD system have also been described by Bhatt (1993) and Mohan *et al.* (1991). From Palomer charts we find that there are two nebulus clouds in the cluster region. Therefore, the cluster region was observed in two fields covering both the clouds in the North and South regions (figures 1a and 1b). Multiple exposures were taken with exposure time ranging from 5 seconds to 1800 seconds depending upon the presence of bright stars and filter used and the frames were coadded in order to achieve a total integration time of 60 minutes in U , 40 minutes in B , 20 minutes in V and 5 minutes each in R and I filters. The observing details are given in the table 1. A number of flats were also taken in each passband by observing the twilight sky. Landolt (1983) standard stars were also observed for calibration purposes.

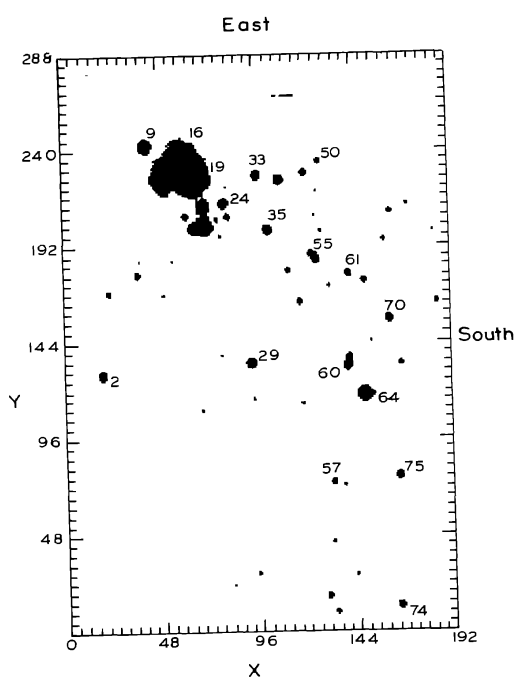


Figure 1a. Identification map for the North region of the cluster NGC 1931.

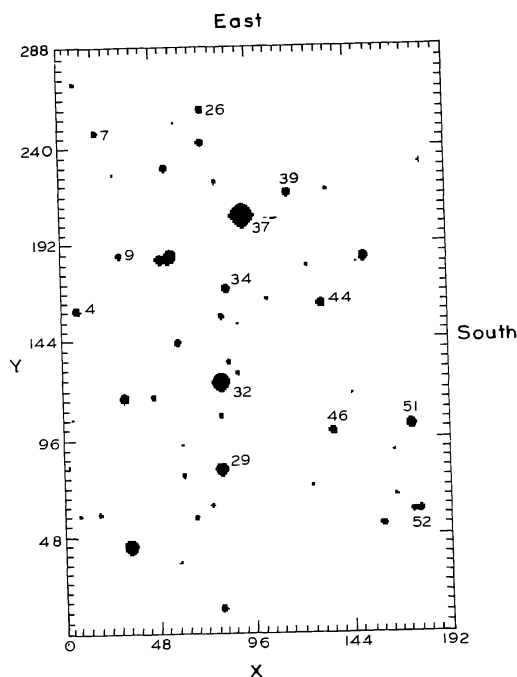


Figure 1b. Identification map for the South region of the cluster NGC 1931.

3. Data reduction

The observations have been reduced using the Micro Vax II system of UPSO. Clean images have been obtained using the ESO MIDAS software package. The cleaned frames in the same filters having similar exposure times were coadded. The photometry was carried out using the DAOPHOT profile-fitting software (Stetson 1987). The stellar point-spread-function (PSF) was evaluated from several uncontaminated stars present in each frame. For a few bright stars which were saturated in the long exposure frames, short exposure frames were used. The X and Y coordinates as well as photometric data of the stars measured in the North and South cluster fields are given in table 2.

Table 1. Details of observations

Filter	North region				South region			
	2/3 Nov 92		12/13 Jan. 93		30/31 Dec. 91		1/2 Nov. 92	
	a	b	a	b	a	b	a	b
<i>U</i>	2	1800	2	300	3	600	2	1800
	1	90			1	300	1	100
<i>B</i>	2	1200	2	120	2	600	2	1200
					1	300	1	60
					1	60		
<i>V</i>	2	600	2	50	2	600	2	600
	1	15			1	300	1	20
					1	60		
<i>R</i>	1	300	1	10	1	300	1	300
	1	10	1	12	1	15	1	5
<i>I</i>	1	300	2	15	1	300	1	300
	1	15			1	20	1	10

Note: Column a and b for each night show the number of frames observed and exposure time in seconds respectively.

Table 2. Magnitudes and colours of the stars in the field of NGC 1931

Star ID	<i>X</i>	<i>Y</i>	$(U - B)$	$(B - V)$	<i>V</i>	$(R - I)$	$(V - I)$	Remark
North Region								
1	6.87	92.95	*	1.150	20.837	1.003	2.199	
2	16.42	124.72	1.067	1.585	15.981	0.996	2.025	
3	20.06	166.92	*	1.364	17.524	0.825	1.822	m
4	32.11	230.40	*	0.525	17.762	0.183	0.881	
5	34.72	176.49	0.426	0.746	16.423	0.501	1.011	m
6	35.73	183.55	*	1.612	18.374	0.897	1.575	
7	38.60	26.79	*	1.125	18.958	0.755	1.538	
8	38.61	98.18	*	1.606	19.929	0.704	1.680	m
9	39.50	244.03	-0.098	0.620	13.971	0.518	0.837	M
10	48.17	166.00	*	1.347	19.157	1.178	2.236	m
11	48.53	222.99	-0.393	0.481	13.019	0.487	0.948	m
12	51.58	208.57	-0.484	0.705	18.105	*	1.046	
13	52.87	183.98	*	1.221	18.771	1.829	1.804	m
14	53.27	151.87	*	1.508	19.763	1.151	2.459	m
15	59.73	206.90	*	1.270	18.243	1.255	2.098	m
16	60.53	236.31	-0.459	0.526	11.447	0.471	0.679	M
17	63.73	200.63	-0.098	0.702	15.645	0.783	1.396	m

Continued

Table 2. Continued

Star ID	X	Y	(U - B)	(B - V)	V	(R - I)	(V - I)	Remark
18	66.00	79.09	-0.837	1.349	19.049	0.784	1.607	
19	66.79	226.54	-0.455	0.496	12.297	0.669	1.003	M
20	67.29	106.60	*	1.606	18.638	0.983	2.091	m
21	69.25	212.39	0.027	0.670	15.332	0.720	1.358	m
22	69.76	200.96	-0.376	0.541	14.119	0.672	1.289	m
23	79.45	95.86	*	1.266	19.707	0.767	1.611	
24	79.68	213.62	-0.074	0.569	15.631	0.543	1.070	
25	81.48	206.71	-0.360	0.795	17.400	0.722	1.395	
26	82.49	15.76	*	1.435	18.445	0.751	1.628	m
27	85.39	89.11	*	1.306	20.706	0.940	1.966	
28	90.93	126.06	*	1.240	19.698	1.296	2.578	
29	92.75	131.11	0.479	1.118	14.971	0.736	1.476	
30	94.04	112.21	*	1.488	18.674	1.059	2.111	m
31	95.17	21.98	*	1.481	18.099	0.819	1.742	m
32	96.20	34.76	*	1.885	19.298	1.045	2.110	
33	96.34	228.30	-0.049	0.457	14.984	0.476	0.919	
34	98.94	25.28	*	1.396	19.562	0.878	1.615	m
35	101.70	200.00	-0.205	0.287	14.499	0.339	0.775	
36	101.88	165.54	*	1.217	19.300	1.009	2.065	m
37	102.99	113.13	*	1.585	19.276	1.006	2.077	m
38	103.93	139.21	*	0.977	19.527	0.743	1.601	
39	107.79	226.00	*	1.970	16.407	1.282	2.583	
40	112.13	178.69	0.430	1.228	17.428	0.800	1.721	m
41	117.76	162.58	0.223	0.843	16.811	0.605	1.278	m
42	118.63	148.84	*	0.850	19.415	0.890	1.710	
43	120.13	207.55	*	1.069	19.551	0.789	1.776	
44	120.60	229.63	0.618	1.207	17.006	0.921	1.714	m
45	123.45	22.40	*	1.741	19.216	0.988	2.007	
46	123.87	187.46	0.837	1.454	17.160	0.890	1.834	M
47	125.91	207.55	*	1.183	18.495	0.800	1.733	m
48	126.37	184.48	0.345	0.535	15.902	0.526	1.104	M
49	126.95	220.23	0.240	0.812	18.325	1.399	1.500	
50	128.14	235.68	0.155	0.760	16.905	0.594	1.055	
51	128.69	199.35	*	1.684	19.178	1.139	2.546	m
52	130.33	189.96	*	1.934	19.875	1.232	2.517	
53	130.75	10.60	0.032	0.828	16.250	0.432	0.949	m
54	132.96	171.04	*	1.444	18.633	1.039	2.093	m
55	133.16	175.16	*	1.162	19.094	0.845	1.583	
56	133.34	38.36	*	1.487	18.202	0.870	1.811	m

Continued

Table 2. Continued

Star ID	X	Y	(U - B)	(B - V)	V	(R - I)	(V - I)	Remark
57	134.00	69.37	0.458	1.086	16.626	0.708	1.456	m
58	136.72	149.82	*	1.326	20.323	0.917	1.784	
59	139.64	67.79	*	1.727	18.509	0.986	1.947	
60	141.66	129.53	0.215	0.702	14.746	0.416	0.919	M
61	142.67	177.35	0.783	0.945	16.711	0.848	1.667	M
62	142.83	133.99	0.821	0.889	16.139	0.608	1.143	M
63	145.23	21.52	*	1.529	18.514	0.970	1.973	m
64	150.24	114.81	-0.341	0.422	12.374	0.313	0.506	M
65	150.66	173.68	0.824	1.200	17.167	0.805	1.659	M
66	152.32	248.50	*	0.910	19.543	0.746	1.873	
67	153.75	142.38	*	1.289	18.414	0.792	1.583	m
68	159.25	173.99	*	1.718	19.566	1.313	2.397	m
69	160.99	195.08	*	1.655	18.905	1.195	2.523	m
70	163.43	154.01	0.441	0.939	15.840	0.617	1.340	M
71	164.21	209.57	0.585	1.038	17.477	0.712	1.541	m
72	165.04	199.77	*	1.414	20.317	1.325	2.424	m
73	165.27	54.98	*	0.936	18.871	0.448	1.457	
74	167.13	5.57	0.203	0.668	15.421	0.381	0.816	m
75	167.54	72.79	0.301	0.669	15.086	0.420	0.693	M
76	168.92	130.97	0.612	1.007	17.040	0.515	1.144	m
77	169.18	172.09	*	1.156	19.698	0.911	1.663	
78	172.93	213.71	*	1.044	18.117	0.860	1.695	m
79	177.78	194.28	*	1.285	19.587	0.834	1.758	
80	182.67	121.36	*	1.825	19.966	1.073	2.087	m
81	185.83	199.52	*	0.931	18.443	0.703	1.527	
82	187.60	163.09	*	1.168	17.608	0.806	1.747	m
83	187.65	169.41	*	1.251	19.725	1.285	2.575	m
84	188.34	179.93	*	1.348	20.077	1.305	2.660	m
South region								
1	2.31	85.38	0.268	0.759	18.023	0.465	0.845	
2	4.51	109.94	0.162	0.477	18.243	0.646	0.938	
3	7.24	60.16	-1.361	1.434	18.547	0.823	1.605	
4	7.92	166.33	0.376	0.725	15.807	0.511	0.854	m
5	9.13	283.56	*	2.005	18.650	0.971	1.825	m
6	17.17	60.78	*	1.255	18.252	0.857	1.586	m
7	19.84	257.88	*	1.622	17.698	0.962	1.768	
8	27.86	236.62	*	1.449	19.397	1.215	2.217	m
9	30.28	194.79	*	2.094	18.140	1.259	2.345	m
10	31.11	120.75	0.369	0.991	15.225	0.642	1.139	M
11	32.23	191.58	*	1.602	19.466	0.953	1.710	m

Continued

Table 2. Continued

Star ID	X	Y	(U - B)	(B - V)	V	(R - I)	(V - I)	Remark
12	32.49	43.91	0.229	0.498	13.056	0.407	0.660	m
13	42.05	64.30	*	1.728	20.233	0.799	1.447	m
14	44.09	191.24	*	1.349	19.582	0.860	1.672	m
15	46.20	121.13	0.352	1.087	17.364	0.662	1.227	m
16	46.21	55.23	*	0.849	19.305	0.924	1.533	
17	51.05	192.36	0.354	0.932	15.428	0.649	1.144	M
18	54.54	239.79	*	1.648	17.422	1.001	1.908	
19	56.48	194.33	-0.318	0.427	13.477	0.305	0.531	m
20	57.67	35.21	*	1.219	18.323	0.698	1.289	m
21	59.18	149.31	0.656	1.115	16.527	0.606	1.162	M
22	60.61	80.33	*	1.522	18.303	0.974	1.856	m
23	60.76	96.08	*	1.436	18.850	0.923	1.708	m
24	66.70	58.60	*	1.647	18.276	1.029	1.951	m
25	73.65	252.37	0.711	0.947	16.613	0.728	1.277	m
26	73.92	269.73	*	1.251	16.444	0.644	1.348	m
27	75.00	64.99	*	0.972	19.467	1.430	2.614	
28	79.07	11.39	*	2.085	17.332	1.203	2.268	m
29	79.96	83.54	0.464	0.694	13.779	0.551	0.926	m
30	80.28	232.08	*	1.238	18.664	1.042	1.880	m
31	80.36	111.11	0.233	0.883	17.680	0.701	1.226	
32	80.81	128.82	-0.378	0.359	11.937	0.263	0.480	M
33	81.75	162.65	*	1.540	17.931	0.970	1.809	
34	84.65	176.80	0.325	0.895	15.528	0.543	1.003	M
35	85.09	139.10	*	1.239	18.560	1.069	2.010	m
36	89.67	133.27	*	0.872	17.847	0.742	1.257	
37	93.65	214.25	-0.486	0.300	11.116	0.286	0.529	M
38	105.55	171.51	*	1.512	19.872	1.490	2.835	m
39	117.21	226.25	0.353	0.934	15.940	0.575	1.139	M
40	118.35	108.50	*	1.405	19.603	1.038	1.714	m
41	126.60	188.54	*	0.955	18.882	0.990	1.737	
42	126.73	74.36	*	1.392	18.582	0.867	1.570	m
43	131.29	116.60	*	1.523	19.610	1.104	1.941	m
44	133.19	168.59	0.299	0.446	15.017	0.402	0.663	
45	137.19	227.47	*	1.172	18.416	0.735	1.504	m
46	137.70	102.37	1.124	1.503	16.784	0.902	1.689	
47	155.44	192.36	0.121	0.425	14.891	0.413	0.748	
48	162.07	63.64	*	1.622	19.716	1.168	2.178	m
49	162.56	54.06	0.669	1.145	16.533	0.605	1.162	M
50	169.17	69.29	*	1.749	19.115	1.241	2.276	
51	177.64	105.25	0.377	0.510	14.414	0.399	0.657	M
52	181.42	61.15	-0.214	1.926	16.674	0.685	1.273	

Notes. *—Observations not available.; m and M—Cluster members (see text)

The cluster fields are observed on different nights. The photometric errors ($\pm \sigma$) of observations are found to be 0.025, 0.030, 0.033, 0.030, 0.019 and 0.023 mag in V , $(B - V)$, $(U - B)$, $(V - R)$, $(R - I)$ and $(V - I)$ respectively. The data have also been compared with the UBV photoelectric photometry of stars by Pandey & Mahra (1986). The mean difference between the two observations and standard deviations (σ) are found to be -0.015 ± 0.030 , -0.007 ± 0.023 and 0.025 ± 0.024 mag in V , $(B - V)$ and $(U - B)$ respectively for the stars having $V < 15.0$ mag.

4. Interstellar extinction

To estimate the interstellar extinction in the cluster region, we have used the $(U - B, B - V)$ diagram shown in figure 2. The intrinsic zero-age-main-sequence (ZAMS) given by Schmidt-Kaler (1982) was fitted to the main-sequence stars of spectral type earlier than A0 in the cluster field. The minimum and maximum reddening values estimated by sliding fit method comes out to be $E(B - V)_{\min} = 0.55$ mag and $E(B - V)_{\max} = 1.00$ mag. The slope $E(U - B)/E(B - V)$ has been taken to be equal to 0.72 (Johnson & Morgan 1953). The observed dispersion in the $E(B - V)$ values cannot be explained due to errors in the data and other parameters such as rotation, duplicity etc. which can produce a maximum variation of 0.11 mag in $E(B - V)$ for MS stars (cf. Burki 1975). Therefore, we conclude that the reddening is non-uniform across the cluster field. The interstellar extinction for individual MS stars has

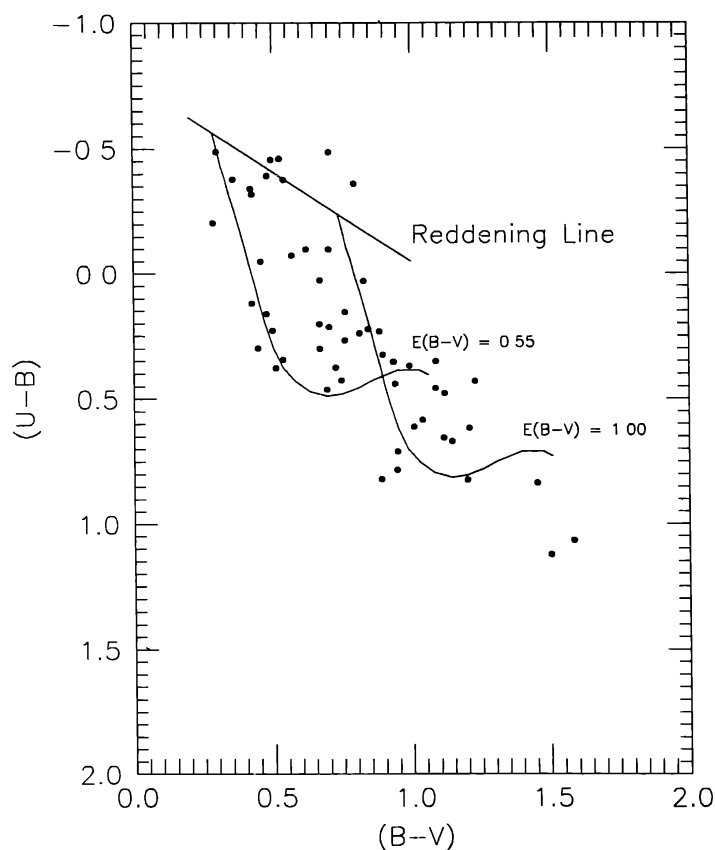


Figure 2. The colour-colour diagram for the stars in the cluster region.

also been derived using the Q-method (Johnson & Morgan 1953). The maximum and minimum values obtained by Pandey & Mahra (1986) are 1.00 and 0.47 mag respectively and which are in close agreement with those obtained in the present study.

5. Distance to the cluster

The colour-magnitude diagrams ($V, B - V$) and ($V, V - I$) are plotted in figures 3 and 4 respectively. A broad but well defined cluster MS is clearly visible up to 20.0 mag. To estimate the distance to the cluster we have fitted the ZAMS given by Schmidt-Kaler (1982) in the ($V, B - V$) colour-magnitude diagram (CMD) and the ZAMS given by Walker (1985) in the ($V, V - I$) CMD) on the bluest envelope of data points in figures 3 and 4 respectively and a distance modulus $(m - M)_v = 14.1$ mag has been obtained for the cluster. We have adopted the relation $E(V - I) = 1.25 \times E(B - V)$ (Walker 1985) to estimate distance modulus from figure 4 and it seems that the slope of 1.25 is valid for this cluster. However, different slopes have been obtained for other clusters, e.g. Bhatt *et al.* (1993) have found a slope of 1.36 for the open cluster NGC 7419 and Alcalá & Ferro (1988) have obtained a value of 1.68 for NGC 7790.

Using the mean $E(B - V) = 0.78$ mag for the cluster, the most acceptable value of $R = 3.1$, $A_v = 3.1 \times 0.78$, the true distance modulus $(m - M)_0$ comes out to be 11.68 mag, which corresponds to a distance of 2.17 kpc. The same value for the distance was obtained by Pandey & Mahra (1986), but in the present work we have confirmed this distance from ($V, V - I$) CMD also.

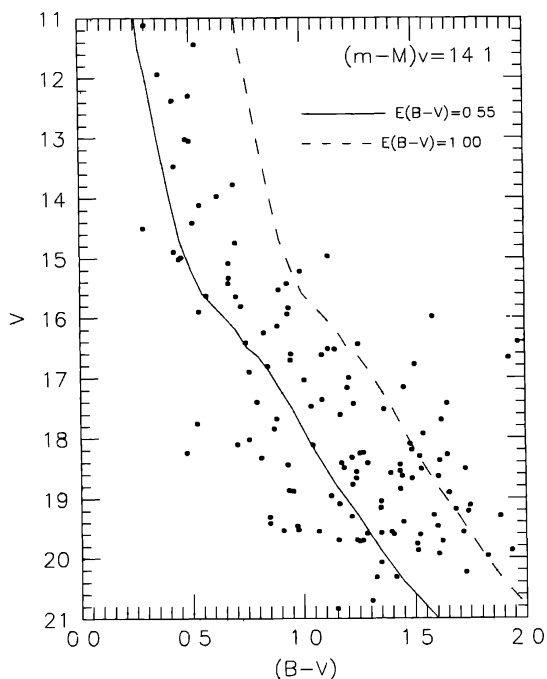


Figure 3. The colour-magnitude diagram ($V, B - V$) for all stars measured in the North and South regions of NGC 1931. The full line and dashed line represent the ZAMS given by Schmidt-Kaler (1982) for minimum and maximum reddening values respectively.

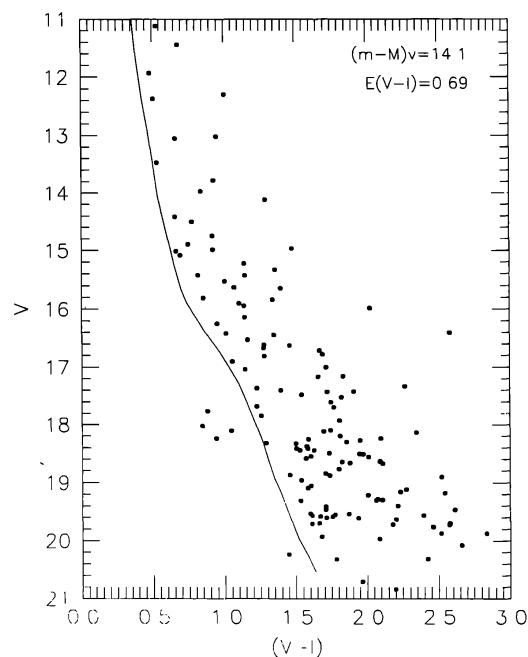


Figure 4. The colour-magnitude diagram ($V, V - I$) for all stars measured in the north and South regions of NGC 1931. The full line represents the ZAMS given by Walker (1985).

6. Membership

Since the proper motion and spectroscopic studies are not available for the stars in the cluster region, the discrimination of non-members from the observed sample has been carried out using the photometric and statistical criteria. We have considered only those stars as members which lie in between blue and the red envelopes of the MS, obtained by shifting the MS for the maximum value of $E(B - V)$ in the $(V, B - V)$ CMD. The stars found inside this belt are designated as 'm' in table 2. The unreddened colour-magnitude diagrams, $(V_0, (B - V)_0)$ and $(V_0, (U - B)_0)$ are plotted in figures 5 and 6 respectively. The main-sequence is drawn and also shifted to 0.75 mag in V_0 with dashed lines in both the CMDs to account for the possible widening of the MS due to binary stars etc. The stars found in this belt are cluster members with a greater probability. These stars are designated as 'M' in table 2.

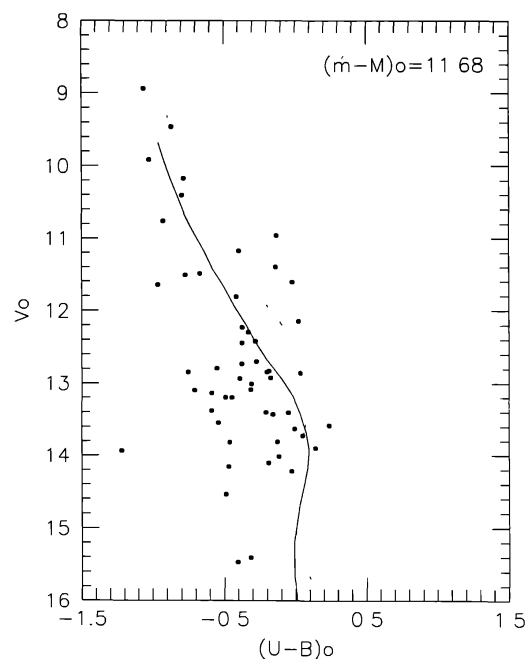
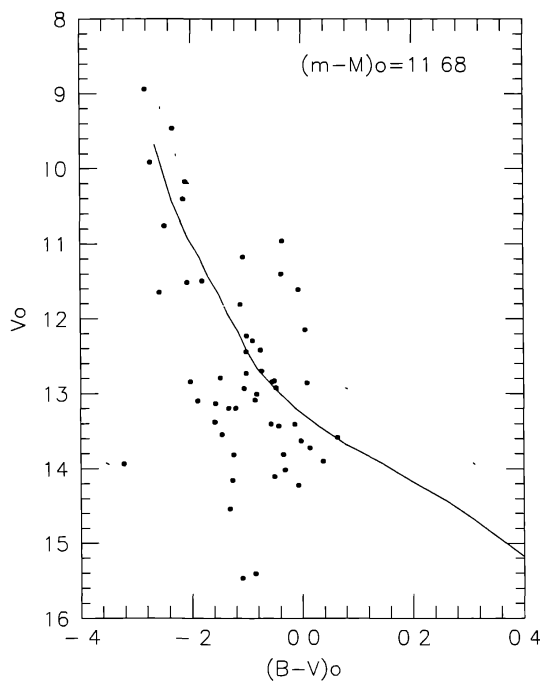


Figure 5. The $(V_0, (B - V)_0)$ diagram of NGC 1931. **Figure 6.** The $(V_0, (U - B)_0)$ diagram of NGC 1931

7. Age of the cluster

To estimate the age of the cluster we have used the observations of those stars for which individual reddening could be obtained. The $(M_v, (B - V)_0)$ and $(M_v, (U - B)_0)$ diagrams for cluster member stars are shown in figures 7 and 8 respectively. The age of the post-main-sequence stars has been estimated using the empirical isochrones given by Mermilliod (1981). From the $(M_v, (B - V)_0)$ and $(M_v, (U - B)_0)$ diagrams it is inferred that the cluster lies between the ages of NGC 6231 and NGC 884 groups. The age of the cluster NGC 6231 and NGC 884 are 0.60×10^7 yr and 1.4×10^7 yr respectively (cf. Maeder & Maynet 1991). The colours of stars at blue turn-off point (in the CMD of NGC 1931) suggest an age $\sim 10^7$ yr (cf. Maeder & Maynet 1991).

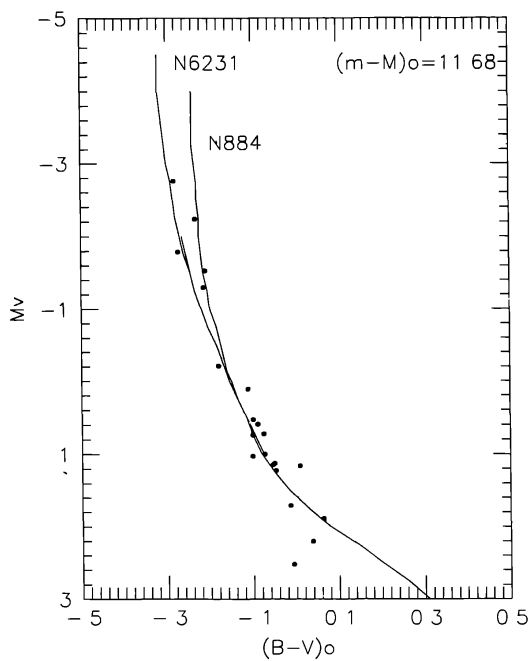


Figure 7. The $(M_v, (B - V)_0)$ diagram of the member stars in NGC 1931.

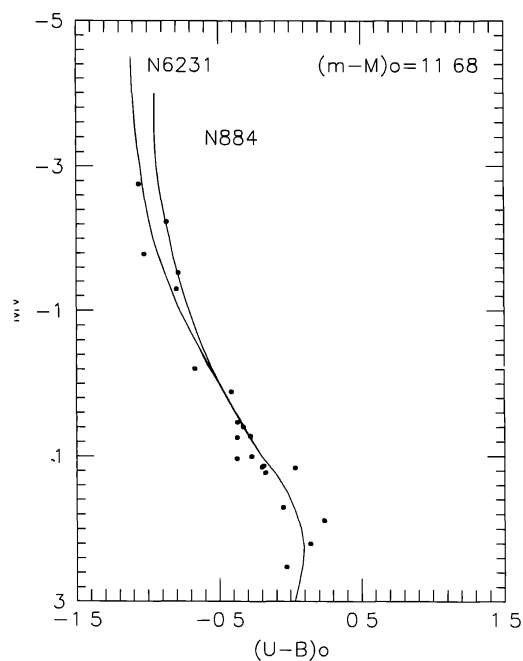


Figure 8. The $(M_v, (U - B)_0)$ diagram of the member stars in NGC 1931.

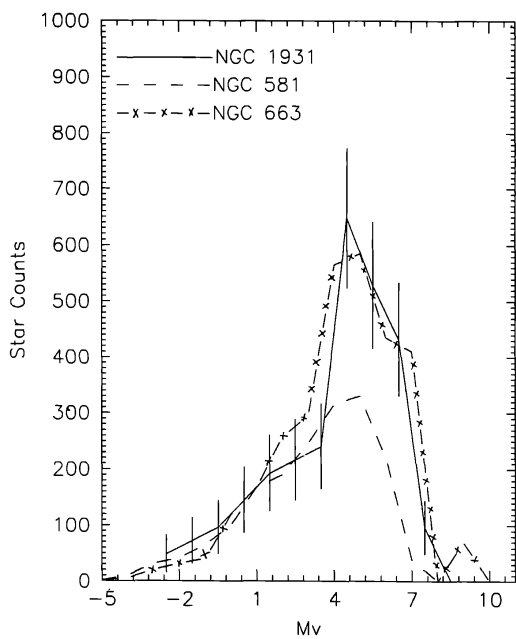


Figure 9. The luminosity function of the cluster stars in NGC 1931. The error bars corresponding to \sqrt{N} are also shown in the figure.

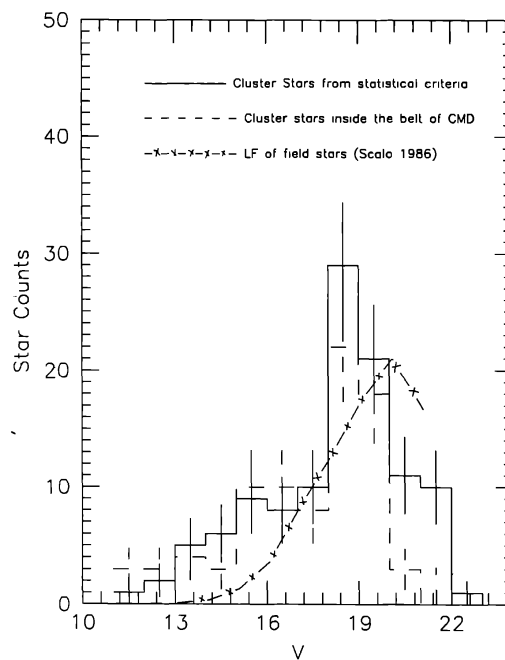


Figure 10. The luminosity distribution of the stars in NGC 1931. The error bars corresponding to \sqrt{N} are also shown in the figure.

8. Luminosity function

We have also observed two field regions located at ~ 30 arc-minute towards East and South directions from the cluster region to estimate the approximate number of field stars present in the cluster region. It is assumed that the distribution of the field stars in the nearby field regions is same as the distribution of field stars in the cluster field. The cluster luminosity function (LF) is then obtained by subtracting the contribution of field stars in each magnitude bin. The luminosity function is shown in figure 9 and a comparison has been made with the LFs of the other young clusters. The data for the clusters NGC 581 and NGC 663 have been taken from Phelps & Janes (1991a, 1991b) and the number of stars were normalized at $M_V = 1.0$ mag. The cluster luminosity functions agree very well towards the higher mass end ($M_V < 4.0$ mag). We believe that $V = 18.0$ mag represents a limit where our photometry is reasonably complete as in the case of NGC 581 and NGC 663. Towards the fainter end the LF of NGC 1931 agrees with that of NGC 581. The distance modulus of NGC 581 is 0.5 mag less than that of NGC 1931. The LF of NGC 1931 is quite different from that of field stars given by Scalo (1986). The LF has also been obtained for the stars which lie in between the blue and red envelopes of MS in the $(V, B - V)$ CMD and a comparison has been made with the LF obtained using the statistical criterion and it is found that both the LFs agree fairly well (figure 10). Thus, it seems that the stars which lie between the two envelopes can be taken as possible members with less uncertainty.

9. Conclusions

The CCD photometry of the cluster NGC 1931 in *UBVRI* photometric passbands down to 20.5 mag indicates a well defined MS of the cluster and a true distance modulus of 11.68 mag corresponding to a distance of 2.17 kpc has been obtained for the cluster. The age of the cluster is estimated to be ~ 10 Myr. The reddening in the cluster region is found to be variable having $\Delta E(B - V) = 0.45$ mag. The LF of NGC 1931 has been compared with the LFs of the two young open clusters NGC 581 and NGC 663 and it is found that LF of NGC 1931 agrees fairly well with the LFs of NGC 581 and NGC 663 towards the higher mass end, however, the LF of field stars given by Scalo (1986) is significantly different.

References

- Alcala J. M., Ferro A. A., 1988, *Rev. Mexi. Astr. Astrof.*, 16, 81
 Bhatt B. C., 1993, Ph.D. thesis, Kumaon University, Naini Tal.
 Bhatt B. C., Pandey A. K., Mohan V., Mahra H. S., Paliwal D. C., 1993, *BASI*, 21, 33.
 Burki G., 1975, *A&A*, 43, 37.
 Johnson H. L., Morgan W. W., 1953, *ApJ*, 117, 313.
 Landolt A. U., 1983, *AJ*, 88, 439
 Lynga G., 1987, *Catalogue of Open Clusters. I/I C7030*, Centre de Donnes Stellaires, Strasbourg.
 Maeder A., Maynet G., 1991, *A&A*, 89, 451.
 Mermilliod J. C., 1981, *A&A*, 97, 235.
 Mohan V., Paliwal D. C., Mahra H. S., 1991, *BASI*, 19, 235
 Moffat A. F. J., Fitzgerald M. P., Jackson P. D., 1979, *A&AS*, 38, 197.
 Pandey A. K., Mahra H. S., 1986, *Ap. Space Sci.*, 120, 107.

- Phelps R. L., Janes K. A., 1991a, in Precision Photometry: Astrophysics of the Galaxy, ed. A G. Davis Philip, L. Davis Press, Schenectady, p 331.
- Phelps R. L., Janes K A , 1991b, Mem. Soc. astr. ital., 62, 507
- Scalo J. M , 1986, Funda. Cosmic Phys , 11, 1
- Schmidt-Kaler Th., 1982, Landolt-Bornstein, Numerical Data and Funct. Relationship in Sci and Tech. New Ser., Group 6, Vol. 2b, p 1.
- Stetson P. B , 1987, PASP, 99, 191.
- Walker A R., 1985, MNRAS, 213, 889.